Ingeniería. Revista de la Universidad de Costa Rica
ISSN: 1409-2441
marcela.quiros@ucr.ac.cr
Universidad de Costa Rica
Costa Rica

Chavez Hernandez, Jose Alexander; Landaverde Quijada, José Miguel; Ayala Valdez, Oscar Edgardo; Mendoza Mejia, Lesly Emidalia

APPLICATION OF CONSTITUTIVE MODELS IN THE VOLCANIC TEPHRA “TIERRA BLANCA JOVEN”

Ingeniería. Revista de la Universidad de Costa Rica, vol. 24, núm. 2, agosto-diciembre, 2014, pp. 53-78
Universidad de Costa Rica
Ciudad Universitaria Rodrigo Facio, Costa Rica

Ingeniería 24 (2): 53-78, ISSN: 1409-2441; 2014. San José, Costa Rica

APPLICATION OF CONSTITUTIVE MODELS IN THE VOLCANIC TEPHRA "TIERRA BLANCA JOVEN"

APLICACIÓN DE MODELOS CONSTITUTIVOS EN LA TEFRA VOLCÁNICA TBJ

Jose Alexander Chavez Hernandez
José Miguel Landaverde Quijada
Oscar Edgardo Ayala Valdez
Lesly Emidalia Mendoza Mejia

Abstract

The volcanic tephra Tierra Blanca Joven (TBJ) covers most of the Metropolitan Area of San Salvador where problems of mass wasting problems occur. To understand its behavior the Mohr-Coulomb, Modified Cam Clay and Hypoplasticity constitutive models were used to simulate consolidation and triaxial tests; looking for the one closer to real laboratory results. The constitutive models are used into finite element software to simulate the behavior of a soil mass (slope stability, bearing capacity etc.). Shear box, drained triaxial and consolidation tests were made in order to obtain the parameters for the models. The soil must be either saturated or dry, otherwise unsaturated properties are needed. After comparing the results of the constitutive model it was observed that none of them display exactly the real behavior observed in the laboratory. Mohr-Coulomb is the model that is used in all the geotechnical studies in El Salvador and it was the model that showed more deficiencies. Hypoplasticity showed good results in the triaxial tests but deviated from reality in the consolidation results. The results indicate that a different constitutive model and lab equipment are necessary (as TBJ is an unsaturated soil) to characterize the behavior of the soils in El Salvador.

Keywords: Constitutive model, hypoplasticity, Tierra Blanca Joven, Mohr-Coulomb, Modified Cam Clay.

Resumen

La tefra volcánica Tierra Blanca Joven (TBJ) cubre la mayoría del Área Metropolitana de San Salvador, donde ocurren problemas de denudación. Para entender su comportamiento los modelos constitutivos Mohr-Coulomb, Cam Clay Modificado e Hipoplasticidad fueron usados para simular pruebas de consolidación y triaxiales; comparándolos con resultados de laboratorio reales. Los modelos constitutivos son usados en programas de elementos finitos para simular el comportamiento del suelo (estabilidad de taludes, capacidad de carga etc.). Pruebas de caja de corte, triaxial drenada y consolidación se realizaron para obtener los parámetros de los modelos. El suelo tiene que estar saturado o seco, sino propiedades de suelo parcialmente saturado son necesarias. Después de comparar los resultados de los modelos constitutivos se observo que ninguno mostro exactamente el comportamiento real observado en laboratorio. Mohr-Coulomb es el modelo que se usa en todos los estudios geotécnicos en El Salvador y fue el que mostro mas deficiencias. Hipoplasticidad mostro buenos resultados en la prueba triaxial pero se desvió de la realidad al compararlo con la consolidación. Estos resultados indican que un modelo constitutivo diferente y equipo de laboratorio es necesario (ya que TBJ es un suelo parcialmente saturado) para caracterizar el comportamiento de los suelos en El Salvador.

Keywords: Modelo constitutivo, hipoplasticidad, Tierra Blanca Joven, Mohr-Coulomb, Cam Clay Modificado.

Recibido: 10 de octubre de 2013 • **Aprobado:** 29 de mayo de 2014

1. INTRODUCTION

Currently the Metropolitan Area of San Salvador (MASS) suffers serious problems of mass wasting processes in the urban areas and edges of streams (Chavez, Hernandez & Kopecky, 2012), which are connected with the properties of the geological layers and inappropriate land use. This problematic is significant during the rainy season or earthquakes; producing environmental, social and economic losses each year. More affected areas belongs to areas with important thickness of Tierra Blanca Joven (TBJ) which is a volcanic tephra, product of the last plinian eruption of the Ilopango caldera that covers most of the surface of the MASS.

TBJ is composed by fall, surge, ash flows and pyroclastic flows deposits. The units that compose TBJ (Chavez et al., 2012), from the base to the surface, are: Ao, A, B, C, α, β, D, F and G (see Figure 1). The change of consolidation, thickness, distribution, grain size and cementation of TBJ

depends of the distance from the Ilopango caldera, type of deposit and deposition. The fall deposits are more unconsolidated, and compared with the pyroclastic flows have more percentage of fines (Hernandez, 2004).

The G unit of TBJ being the closest to the surface has been more studied. Authors like Guzman & Melara, (1996); Amaya & Hayem, (2000); Hernandez, (2004); Rolo et al., (2004); Molina, Perez & Vasquez, (2009); Avalos & Castro, (2010) have obtained some physical and mechanical properties of TBJ "G" unit. Results of cohesion and friction angle are usually reported, but scatter in the results are observed (Figure 14 of Chavez, Valenta, Schröfel, Hernandez & Šebesta, 2012); these differences are connected to the stress state, studied unit and moisture content.

Under shear stress, soils behave like is displayed in Figure 2. An elastic region is followed by a peak (if overconsolidated); subsequently a zone is reached (after approximate 10% of strain), where shearing takes place at constant volume (critical or ultimate state). If the tested soil is a clay, then after experimenting great deformation a residual stress is observed (residual state) showing laminar flow (Craig, 2004; Atkinson, 2007). To represent the soil behavior explained above, several constitutive models are available, each one attempt to emulate the reality.

The constitutive models (Murray & Sivakumar, 2010) connect the volume changes and shear stress in a soil and can be applied into the whole range of expected stresses. They provide a qualitative framework to improve the understanding of soil behavior. The constitutive models are used into finite element software to simulate the behavior of a soil mass (slope stability, bearing capacity etc.).

The aim of this paper is to evaluate (into the frame of classical soil mechanics for saturated soils) three constitutive models that can represent the soil behavior (Mohr-Coulomb, Modified Cam Clay and Hypoplasticity) and start understanding the behavior of a volcanic tephra. For this reason comparisons were made between lab results (drained triaxial and consolidation tests) and simulations of the tests in a finite element program (PLAXIS) using the models. The soil must be either saturated or dry; otherwise unsaturated soil mechanics are needed.

TBJ is an unsaturated soil (Chavez et al., 2012a and Chavez, Šebesta, Kopecky, Lopez &Landaverde, 2013); this mean that capillary forces (suction) on the soil structure make that an "apparent cohesion" improves the strength of the soil, also cementation could be important. This condition makes that the slopes are almost vertical and temporally stable, but will collapse when wetted or during earthquakes. Ordinarily, the two independent stress variables used (Fredlund & Rahardjo 1993; Murray & Sivakumar 2010) are the net stress σ-ua and matric suction ua-uw. Being total stress σ, pore water pressure uw and pore air pressure ua. For this reason a proper understanding of the behavior and special characteristics of unsaturated soils are essential, in order to recommend the design criteria for slopes, foundations, road pavements, retaining structures, embankments, groundwater and pollutant flows.

The classical soil mechanics for saturated soil is applied in El Salvador, and the Mohr–Coulomb (plastic failure) constitutive model is extensively used, which is a linear elastic perfectly plastic model.

There are other constitutive models, for example the elasto-plastic models (e.g. Modified Cam Clay) that use the critical state concept, but a state boundary surface is needed to separate the elastic and plastic behavior. The state boundary surface is a frontier to all possible states of a reconstituted soil (Atkinson, 2007), but soils with cementation or suction can occur outside of this boundary. Also it has been proven that nonlinear behavior can take place inside the state boundary surface.

Hypoplasticity for sands (von Wolffersdorff, 1996) is the other model verified in this paper. According to (Herle & Gudehus 1999) the hypoplastic law is a good choice for cohesionless soils because it describes the behavior of soil very realistic; it also associates the strain rate to the stress rate. According to Anaraki (2008) in hypoplasticity is not necessary a yield surface or a decomposition of strain rate into elastic and plastic portions.

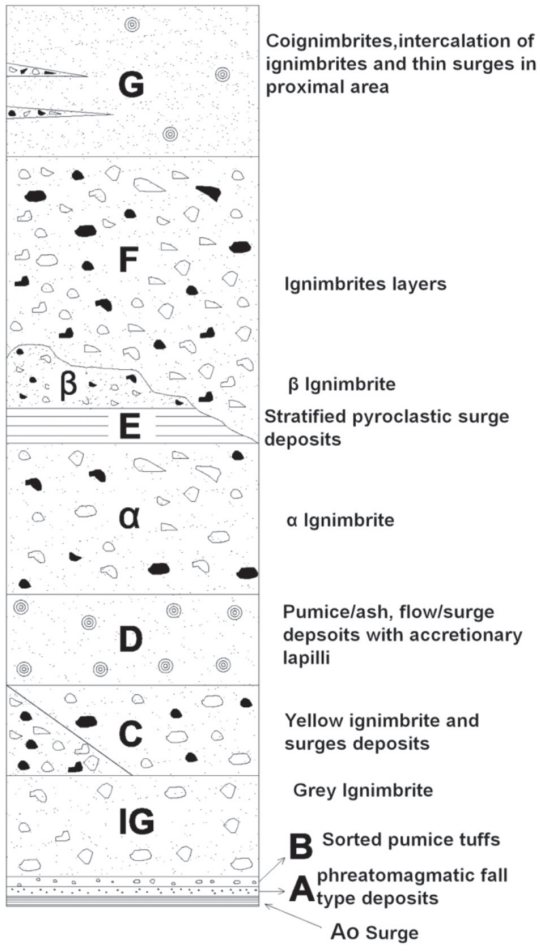

Figure 1. Units that compose Tierra Blanca Joven

Note: Adapted from "Características Geotécnicas y Vulcanológicas de las tefras de Tierra Blanca Joven, de Ilopango, El Salvador " by W. Hernández, 2004, Tesis de Maestría en Tecnologías geológicas, Universidad Politécnica de El Salvador, San Salvador.

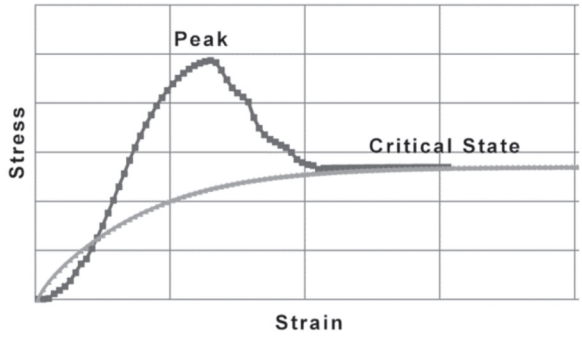

Figure 2. Behavior of soil (sand or silt) under shear stress.

2. METHODOLOGY

The parameters for the models were obtained running tests on the shear box and oedometer in the laboratory of the Universidad de El Salvador (UES). The drained triaxial tests were performed in a private laboratory (Suelos & Materiales) under supervision of the authors of this paper.

To simulate the basic geotechnical tests, the *SoilTest* option of the software PLAXIS VIP (License of Czech Technical University, ČVUT) was used. PLAXIS has already incorporated some standard models (e. g. Mohr-Coulomb, Modified Cam Clay); but also there´s the possibility to run user-defined models (e.g. Hypoplasticity, provided upon request by PLAXIS).

The studied layer (identified as Padre Arrupe) correspond to a fall deposit of TBJ "G" unit (13° 43'1.42''N ; 89° 09'33.77''W) and is presented in Figure 3. The grain size curves of three points of "G" fall deposits are presented in Figure 4 and 5. The change of grain size depends of the distance from the Ilopango caldera. Since the Padre Arrupe point is more distant then there´s more presence of fines than the Bosques de la Paz point. The fall deposit of G unit was classified (SUCS classification) as sandy silt. Additionally, it was not possible to attain the Atterberg limits (liquid limit and plastic limits).

To obtain the parameters for the constitutive models it was necessary to test the soil in different states: saturated (to avoid capillary forces or suction in the drained triaxial test), dry (to avoid capillary forces (suction) in the consolidation and shear box tests), loose (for maximum void ratio and obtain the critical void ratio) and dense (for obtaining stiffness parameters and minimum void ratio).

To achieve the loosest state for the consolidation tests, first the soil was put in the drying oven for 24 hours with a temperature of 110 ± 5 °C. Then the consolidation ring and porous stone was assembled and measures were taken to obtain the volume and weight of the set. Afterwards the dry soil was placed into the ensemble (consolidation ring and porous stone) using a funnel leaving a small drop height for the soil. Next, leveling and filling of voids was needed. The weight was used to obtain the volumetric dry weight (chosen range of dry density was between 0.79-0.86 g/cm^3). A similar process was used with the shear box.

For the densest state in the consolidation tests: the soil was put in the drying oven for 24 hours with a temperature of 110 ± 5 °C. Then consolidation ring and porous stone was assembled and measures were taken to obtain the volume and weight. Afterwards the dry soil was placed into the ensemble (consolidation ring and porous stone) using a funnel and compacting manually, using the porous stone and the load distribution plate of the oedometer. Compaction was made for two layers, pressing five times as harder as possible. Next, leveling and filling of voids was needed. Also a kinetic compaction was prepared for the sample, and in this method a steel rod (30 cm height and 2.54 cm of diameter) was dropped 50 times from a height of 20 cm. Afterwards the whole set was put into a vibrating table for 1 minute (5000 rpm) with a load of 20 kg. Next, leveling and filling of voids was needed. The weight was needed to obtain the volumetric dry weight (chosen range of dry density was between 1.13-1.16 g/cm^3).

For the overconsolidated triaxial tests, the procedure described in Proctor ASTM D-1557 was followed. The optimum moisture was of 20.2 % and the maximum dry volumetric weight was 1435 kg/m^3.

2.1 Mohr-Coulomb

The Mohr-Coulomb constitutive model is a first order approximation to the nonlinear soil behavior. This model is only recommended for a first analysis of the measured situation (Material Models Manual of PLAXIS, 2012). Is composed by the Hooke's law (elastic) and the Mohr-Coulomb failure criterion (plastic). With this model is possible to simulate the behavior of normally consolidated fine or granular soils. The basic theory of this model is explained in Potts & Zdravković (1999).

The Mohr-Coulomb model has 5 parameters: The Young´s modulus (E), The Poisson's

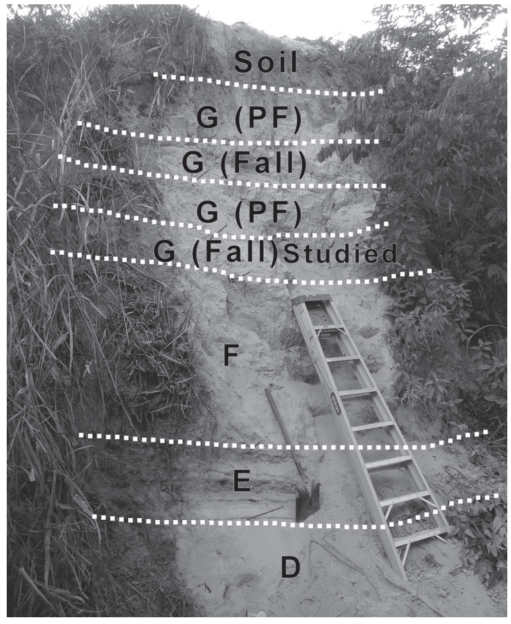

Figure 3. Slope of TBJ with the studied layer (Unit G, fall) in Padre Arrupe.

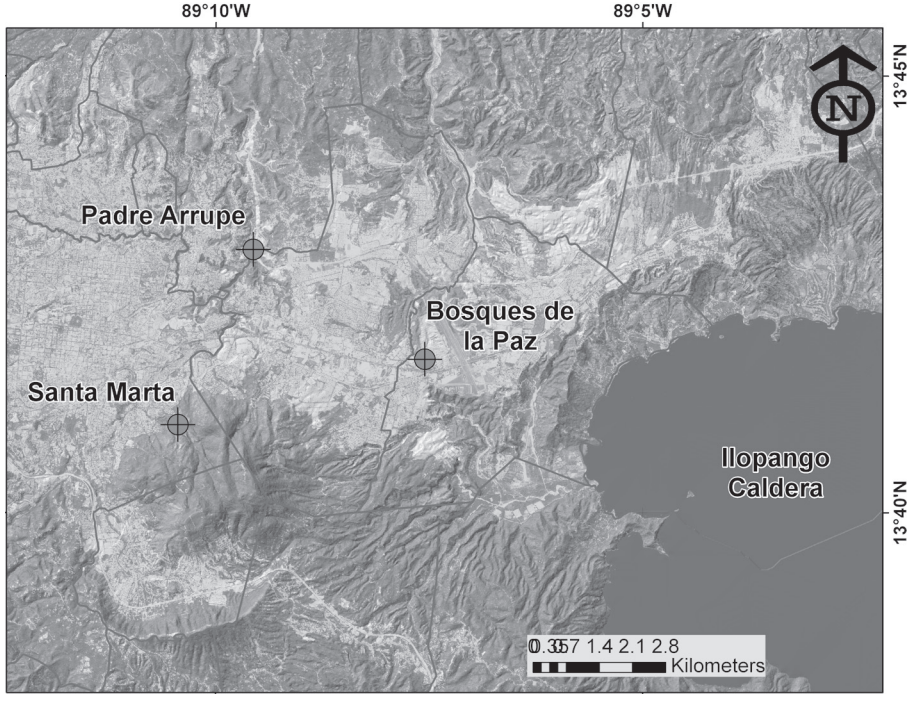

Figure 4. Points with TBJ with the studied layer (Unit G, fall)

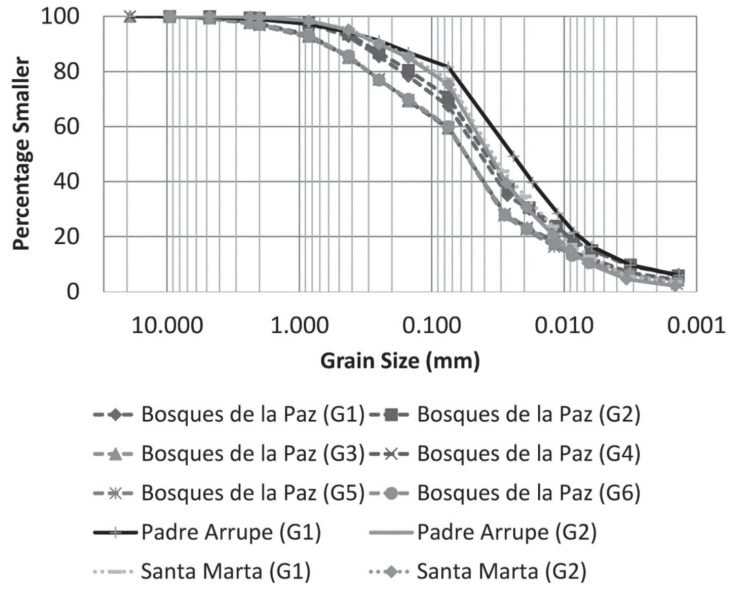

Figure 5. Grain size curve of G fall layers of Figure 4.

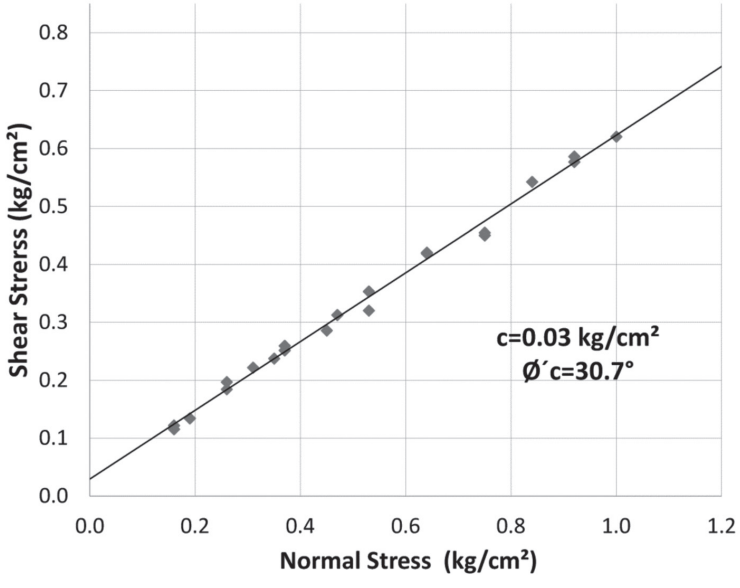

Figure 6. Shear box final failure results.

ratio (υ), cohesion (c), friction angle ($\varphi'c$) and the dilatancy angle (Ψ). The two first ones are related to the elasticity of the soil and the others with the plasticity and dilatancy respectively.

Values of friction angle ($\varphi'c$) and cohesion (c) were obtained using the shear box test in remolded, dried samples in the loosest state possible. The reason for this modifications in the tested samples, were to avoid the natural capillary forces and cementation, and make sure that the critical state (Craig, 2004; Atkinson, 2007) is reached (see Figure 6).

Furthermore, the friction angle ($\varphi'c$) and cohesion (c) were obtained using also the drained-consolidated triaxial test. But the samples were saturated (to avoid the natural capillary forces and cementation). Undisturbed samples were used (normally consolidated) to compare with the shear box results and to make sure that the critical state was reached (see Figure 7 and Table 1). Remolded samples (dense sample using the Proctor test ASTM D-1557) were tested as well, with the drained triaxial apparatus (see Figure 8 and Table 2).

The Young´s (Elasticity) modulus (E) comes from the stress-strain curve (see Figure 7 and 8) of the drained triaxial tests. The secant modulus at 50% strength is denoted as E_{50} and was the base for obtaining the elastic segment line. Being the Young´s modulus (E) the slope of this line.

$$E_{50} = \frac{\sigma_{max(50\%)} - \sigma_{origin}}{\varepsilon_2 - \varepsilon_1} \quad (1)$$

Where:

$\sigma_{max(50\%)}$: Represents 50% of maximum stress of the curve: σmáx*(0.5).

σ_{origin} : Value of the origin stress, σ = 0.0 kPa.

$\varepsilon_2, \varepsilon_1$: Strain in mm/mm of stress at 50% of maximum and origin, respectively.

The Poisson´s ratio (υ) comes from the curve of volumetric strain-axial strain of the drained triaxial tests and the equation is:

$$\upsilon = \frac{1}{2}\left(1 - \frac{\varepsilon_V}{\varepsilon_a}\right) \quad (2)$$

Where:

$\frac{\varepsilon_V}{\varepsilon_a}$: Represents the slope of the volumetric strain-axial strain curve (elastic segment).

The dilatancy angle (Ψ) can be approximated as $\Psi = \varphi - 30°$ (Material Models Manual of PLAXIS, 2012).

The parameters used for the Mohr-Coulomb model are summarized in Table 3. For cohesion (c) and friction angle ($\varphi'c$) the results of the drained triaxial test were selected.

2.2 The Modified Cam Clay

The Modified Cam Clay is based on the critical state theory (Craig, 2004; Atkinson, 2007) and is recommended for modeling near normally consolidated fine soils (Material Models Manual of PLAXIS, 2012). The critical state theory try to represent the elasto-plastic behavior of the soil using the normal and shear stresses, but also including a parameter that associates the volumetric changes of the material.

The boundary surface of the Modified Cam Clay is an elliptic surface where the soil yields. The equation is (Camacho, Reyes & Bueno, 2004):

$$\frac{p'}{p'_o} = \frac{M^2}{M^2 + \eta^2} \quad (3)$$

Where:

$$\eta = \frac{q}{p'}$$

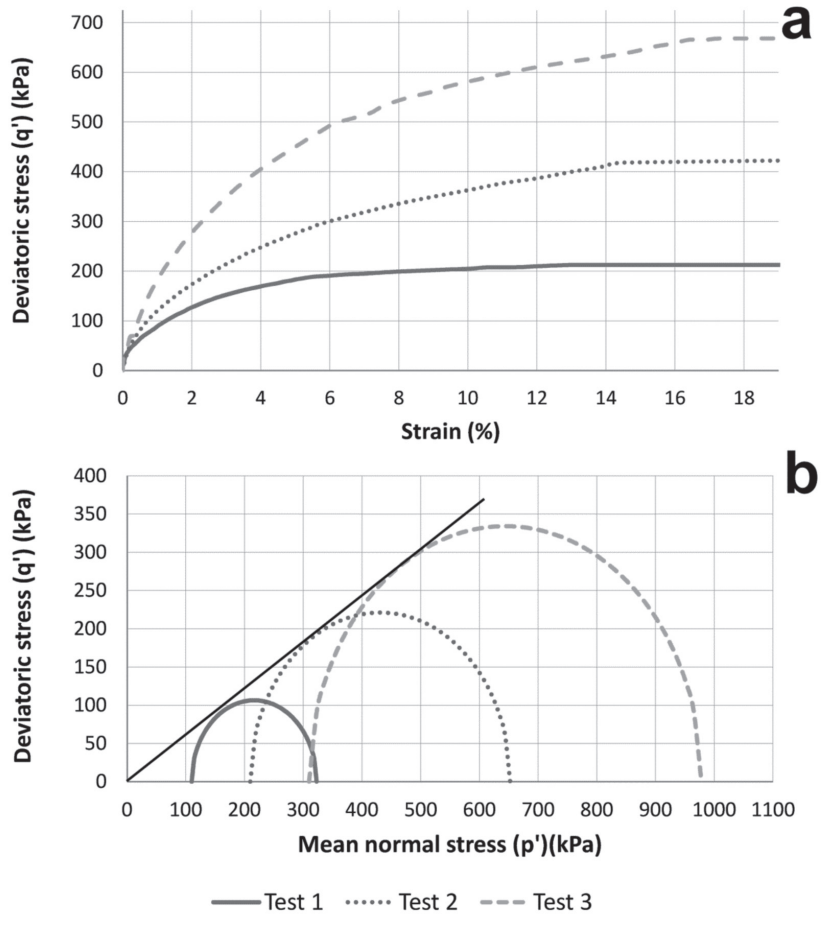

Figure 7. (a)Stress-strain curve of undisturbed samples with the drained triaxial tests. (b) Mohr-Coulomb failure criteria.

$p´_o$ is the stress that controls the size of the boundary surface; $q= \sigma1-\sigma3$ and $p´= 1/3(\sigma1+2\sigma3)$. M is the slope of the critical state line (CSL) that controls the shape of the boundary surface (Atkinson, 2007). When $p´$ and q are located in the interior of this surface, only elastic strains are expected, but once the stress path reaches the boundary surface (ellipse) the plastic deformations begin.

The Modified Cam Clay model has five parameters: swelling or unloading slope ($\varkappa$); compression or loading slope (λ); (M) as tangent of the Critical State Line (CSL); the Poisson´s ratio (υ) and the specific volume in a unitary effective stress (Γ). PLAXIS uses the initial void ratio (e_i) instead of Γ. The hardening law of this model (Camacho et al., 2004) indicates the magnitude of plastic deformations and the change of the boundary surface. The size of the boundary surface depends of $p´_o$, but this value is not constant and is linked to the plastic volumetric strain:

$$\frac{\delta p´_o}{\delta \varepsilon_p^p} = \frac{\upsilon . p´_o}{\lambda - \kappa} \tag{4}$$

Where $\delta\varepsilon_p^p$ is the increment of volumetric plastic strain and $\delta p´_o$is the increment of stress.

Table 1. Undisturbed triaxial tests information.

	Test 1	Test 2	Test 3
Initial Moisture Content (%)	16.44	16.72	17.05
Final Moisture Content (%)	41.43	41.89	42.04
Initial Dry Volumetric Weight (g/cm^3)	1.007	1.016	1.019
Final Dry Volumetric Weight (g/cm^3)	1.115	1.134	1.139
Initial Void Ratio	1.394	1.372	1.366
Final Void Ratio	1.161	1.125	1.117
Specific gravity	2.42	2.42	2.42
q (kPa)	212.69	442.32	667.95
Confinement Stress (kPa)	110	210	310
Øc (degrees)		30.90	
Cohesion (kPa)		1.34	

Table 2. Disturbed (dense) triaxial tests information.

	Test 1	Test 2	Test 3
Initial Moisture Content (%)	18.99	19.2	19.39
Final Moisture Content (%)	26.96	26.9	27.08
Initial Dry Volumetric Weight (g/cm^3)	1.419	1.417	1.41
Final Dry Volumetric Weight (g/cm^3)	1.488	1.482	1.541
Initial Void Ratio	0.698	0.701	0.709
Final Void Ratio	0.62	0.626	0.564
Specific gravity	2.42	2.42	2.42
q (kPa)	1223.7	1939.5	2450.8
Confinement Stress (kPa)	100	200	300
Øc (degrees)		50.10	
Cohesion (kPa)		97.01	

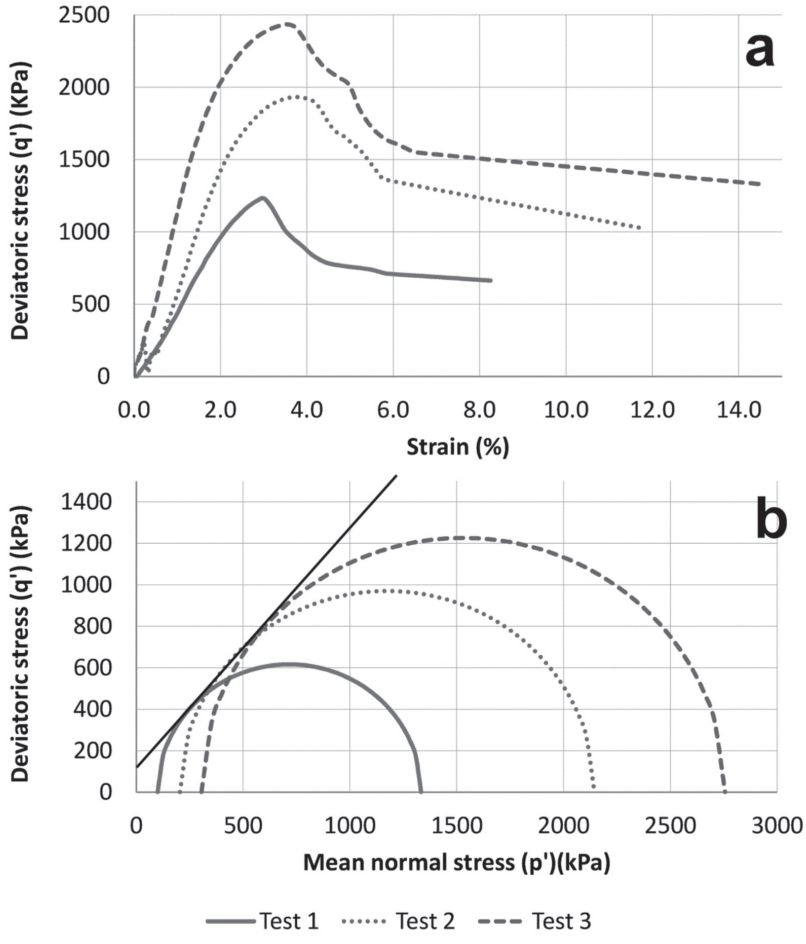

Figure 8. (a)Stress-strain curve of disturbed samples (dense) with the drained triaxial tests. (b) Mohr-Coulomb failure criteria.

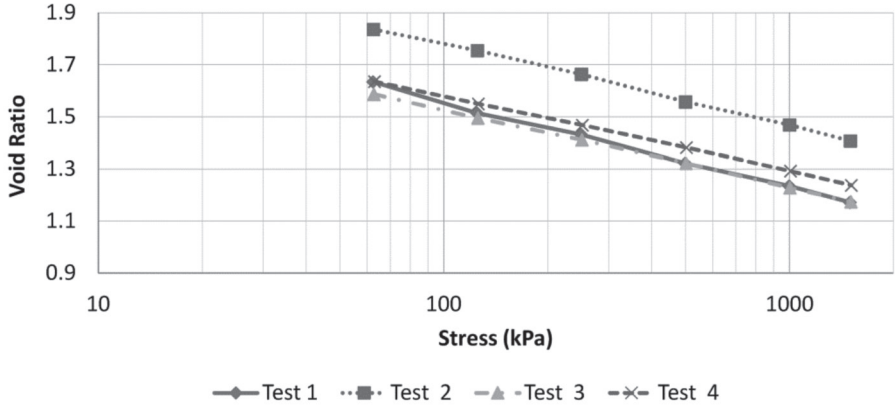

Figure 9. Consolidation tests of loose samples

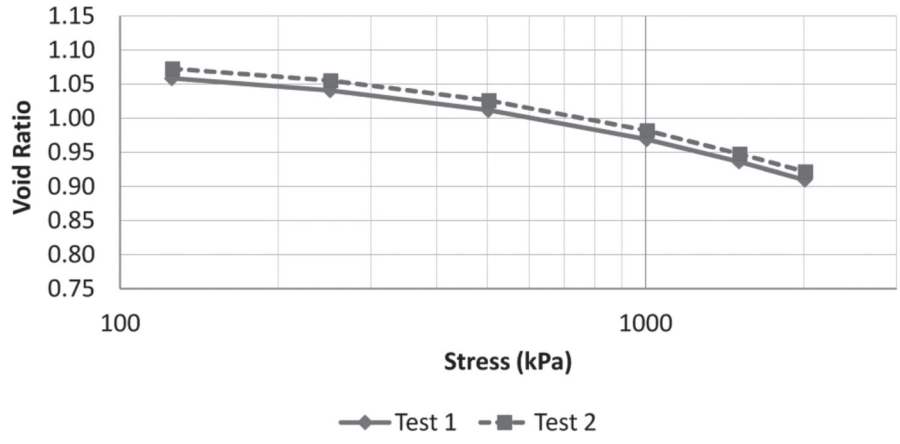

Figure 10. Consolidation tests of dense samples

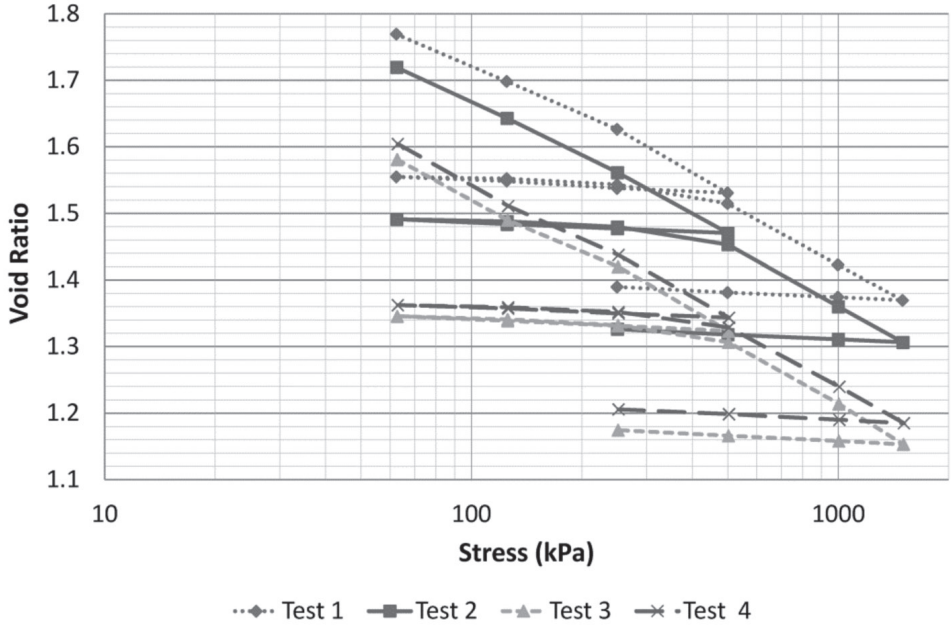

Figure 11. Consolidation load-unload tests of loose samples

In Figure 9, 10 and 11 load, load-unload consolidation results are presented. The Normal Consolidation Line (NCL) and the Critical State Line (CSL) are parallel (Atkinson, 2007), with a slope λ. The unloading slope ϰ is also represented in the load-unload consolidation graphic (see Figure 12).

M in the space *q-p´* can be obtained directly from the graphic (see Figure 13) that includes the critical state points of the undisturbed drained triaxial tests, but is also found (Atkinson, 2007) using the critical friction angle (φ*c*):

$$M = (6 \sin \varphi c) / (3 - \sin \varphi c) \quad (5)$$

A similar value of *M* was obtained using the graphic of Figure 13 (1.23) and Equation 5 (1.24), this means that the critical state was reached in the undisturbed triaxial tests.

The Poisson´s ratio (υ) values are the same as explained before in the Mohr-Coulomb model.

Consolidation tests were made in dense and loose states; also load-unload consolidation tests were required (loose state). The tests were made in dry remolded samples to avoid the natural capillary forces (or suction) and cementation, and make sure that the critical state is reached.

In Table 4, 5 and Figure 9 the results of the consolidation tests made in the loosest state are presented. Test 2 was chosen for simulation.

In Table 6, 7 and Figure 10 are the results of the consolidation tests made in the densest state. Test 1 was chosen for simulation.

In Table 8 and 9 and Figure 11 are the results of the consolidation tests made for the load-unload tests. Test 2 was chosen for simulation.

In the Equations 6 and 7 (Atkinson, 2007) λ and k have a relationship with the slope of the NCL of the load segment of a consolidation test (C_c) and with the load-unload segment (C_S). The denominator 2.3 is related with the fact that the stress axis of Figure 12a is in Ln and the consolidation test (see Figure 12b) is in Log_{10}.

$$\lambda = \frac{C_c}{2.3} \quad (6)$$

$$\kappa = \frac{C_s}{2.3} \quad (7)$$

$$C_c = \frac{\Delta e}{\Delta \ln \sigma_z} \quad (8)$$

$$C_s = \frac{\Delta e}{\Delta \ln \sigma_z} \quad (9)$$

The initial void ratio (e_i) parameter corresponds to the test to be simulated.

The parameters used for the Modified Cam Clay model are summarized in Table 10.

Table 3. Parameters used for the Mohr-Coulomb model.

	Critical Friction Angle φ´c (degrees)	Cohesion c (kPa)	Elasticity Modulus E (kPa)	Dilatancy Angle Ψ (degrees)	Poisson Modulus υ
Normally consolidated	30.9	1.34	8757.2	0	0.3675
Overconsolidated	50.1	97.01	110454	20.13	0.4604

Table 4. Information of loose consolidation tests.

	Test 1	Test 2	Test 3	Test 4
Total Deformation (mm)	5.2175	4.8375	4.8375	4.2975
Initial Dry Volumetric Weight (g/cm^3)	0.82	0.845	0.845	0.851
Final Dry Volumetric Weight (g/cm^3)	1.114	1.118	1.118	1.086

Table 5. Results of loose consolidation tests.

Test 1		Test 2		Test 3		Test 4	
Stress(kPa)	Void Ratio	Stress (kPa)	Void Ratio	Stress (kPa)	Void Ratio	Stress (kPa)	Void Ratio
0	1.95	0	2.06	0	1.87	0	1.84
62.32	1.63	62.52	1.84	62.72	1.59	62.92	1.63
124.65	1.51	125.04	1.75	125.44	1.49	125.84	1.55
249.29	1.43	250.08	1.66	250.88	1.41	251.67	1.47
498.59	1.32	500.17	1.56	501.75	1.32	503.35	1.38
997.18	1.23	1000.34	1.47	1003.51	1.23	1006.7	1.29
1495.77	1.17	1500.5	1.41	1505.26	1.17	1510.05	1.24

Table 6. Information of dense consolidation tests.

	Test 1	Test 2
Total Deformation (mm)	1.89	1.7825
Initial Dry Volumetric Weight (g/cm^3)	1.14	1.153
Final Dry Volumetric Weight (g/cm^3)	1.26	1.267

Table 7. Results of dense consolidation tests.

Test 1		Test 2	
Stress (kPa)	**Void Ratio**	**Stress (kPa)**	**Void Ratio**
0	1.1	0	1.12
125.44	1.06	125.84	1.07
250.88	1.04	251.67	1.06
501.75	1.01	503.35	1.03
1003.51	0.97	1006.7	0.98
1505.26	0.94	1510.05	0.95
2007.02	0.91	2013.39	0.92

Table 8. Information of load-unload consolidation tests.

	Test 1	**Test 2**	**Test 3**	**Test 4**
Total Deformation (mm)	3.5825	4.225	4.75	4.5375
Initial Dry Volumetric Weight (g/cm^3)	0.836	0.827	0.854	0.854
Final Dry Volumetric Weight (g/cm^3)	1.021	1.049	1.124	1.108

2.3 Hypoplasticity

According to Anaraki (2008) hypoplasticity takes into consideration the influence of mean pressure and density along various deformation paths. This constitutive law can describe the deformation behavior of cohesionless soils, including the nonlinearity and inelasticity.

The hypoplastic equation used in this paper (for sands) was elaborated by von Wolffersdorff (1996) and is written as (see equation 10)

Where $\dot{\boldsymbol{T}}_s$ represents the objective stress rate tensors as a function of the current void ratio e, the Cauchy granulate stress tensor Ts and the stretching tensor of the granular skeleton is D. $\hat{\boldsymbol{T}}_s$ is the stress ratio tensor (Anaraki, 2008) (see equation 11)

$\hat{\mathbf{T}}_s^* = \hat{\mathbf{T}}_s - \frac{1}{3}\mathbf{I}$ is the deviatoric part of $\hat{\mathbf{T}}_s$ and $\mathbf{I}$ is the unit tensor.The factor a is determined by the friction angle $\varphi' c$ in critical states (see equation 12)

The factor F^2 is a function (Anaraki, 2008) of the deviatoric stress ratio tensor $\hat{\mathbf{T}}_s^*$ (see equation 13)

$$\hat{\mathbf{T}}_S = \frac{\boldsymbol{T}_S}{tr\boldsymbol{T}_S} \tag{11}$$

$$\dot{\boldsymbol{T}}_s = f_e f_b \frac{1}{tr\hat{T}_s^2}\left(F^2\boldsymbol{D} + a^2 tr\left(\hat{\boldsymbol{T}}_s\boldsymbol{D}\right)\hat{\boldsymbol{T}}_s + f_d aF\left(\hat{\boldsymbol{T}}_s + \hat{\boldsymbol{T}}_s^*\right)\parallel \boldsymbol{D} \parallel\right) \tag{10}$$

$$a = \sqrt{\frac{3}{8}}\frac{(3-\sin\varphi_c)}{\sin\varphi_c} \tag{12}$$

$$F = \sqrt{\frac{1}{8}\tan^2\psi + \frac{(2-\tan^2\psi)}{2+\sqrt{2}\tan\psi\cos 30}} - \frac{1}{2\sqrt{2}}\tan\psi \tag{13}$$

Where:

$$\tan\psi = \sqrt{3}\parallel \hat{\mathbf{T}}_s^* \parallel, \quad \cos 3\theta = -\frac{1}{2\sqrt{2}}\tan\psi \tag{14}$$

The void ratio involved in the constitutive function is determined from the mass balance equation.

$$\dot{e} = (1+e)tr\mathbf{D} \tag{15}$$

The void ratio ec (Mašin, 2011) in the critical state and the corresponding mean pressure $-tr\frac{\mathbf{T}_s}{3}$ ($tr\mathbf{T}_s < 0$ or compression) are assumed to be connected by the relation.

$$\frac{e_{ic}}{e_{c0}} = \frac{e_i}{e_{i0}} = \frac{e_d}{e_{d0}} = exp\left[-\left(\frac{-trT_s}{h_s}\right)^n\right] \tag{16}$$

Where e_{c0}, *hs* and *n* are material constants. Equation 16 describe the critical void ratio for high as well as low pressures. Two other characteristic void ratios are specified as functions of the mean pressure: the minimal void ratio, e_d, and the void ratio in the loosest state, e_i with the corresponding reference values e_{i0}, e_{d0} for zero pressure.

The transition to the critical state (Anaraki, 2008), the peak friction angle and the dilative behavior is controlled by the pycnotropy factor *fd*, where α is a material parameter.

$$f_d = \left(\frac{e-e_d}{e_c-e_d}\right)^{\alpha} \tag{17}$$

The factor *fe* controls the influence of the void ratio *e* on the incremental stiffness, where β is a material parameter.

$$f_e = \left(\frac{e_c}{e}\right)^{\beta} \tag{18}$$

The barotropic factor *fb* was introduced to take into account the increase of the stiffness consecutive to an increase of the mean stress. (see equation 19)

fs is defined as the product of the density factor *fe* and the barotropic factor *fb*. (see equation 20)

In conclusion the model by von Wolffersdorff (1996) requires 8 material parameters (Mašin, 2011): φ´*c* is the critical state friction angle; *hs* and *n* control the shape of limiting void ratio curves (normal compression lines and critical state line); e_{d0}, e_{c0} and e_{i0} are reference void ratios specifying positions of limiting void ratio curves; α controls the dependency of peak friction angle on relative density; β controls the dependency of soil stiffness on relative density.

Calibration procedure for the von Wolffersdorff hypoplastic model is explained by Herle & Gudehus (1999) and Mašin (2011).

A simple estimation of φφ´*c* can be obtained from the angle of repose of a dry sample if cohesive forces are negligible. For TBJ an angle of repose of 37° was obtained, and if compared with the results of shear box and the triaxial tests, a difference of approximately 6° was observed. For this reason, the result of angle of repose was discarded since capillary forces related to air humidity increased the repose angle.

The critical void ratio e_{c0} is related to the critical state. Theoretically it´s defined at zero pressure, but alternatively (Anaraki, 2008) it can be equal to e_{max} corresponding to a loose oedometric specimen. In Table 11 there are the void ratio results of consolidation test made for TBJ in the loosest state.

The void ratios e_{d0} and e_{i0}, can approximately (Mašin, 2011) be obtained from empirical relations. e_{d0} is void ratio at minimum density (e_{min}). The minimum void ratio e_{d0} was obtained by densification of TBJ samples using the method for consolidation test explained at the start of methodology section (see Table 12). If it´s not possible to have a dense sample, then e_{d0} can be approximated with $e_{d0}=e_{c0}*(0.4)$.

Void ratio e_{i0} represents (Anaraki, 2008) the maximum void ratio at zero pressure (isotropic consolidation of a grain suspension in a gravity free space). Void ratio e_{i0} can be approximated with $e_{i0}=e_{c0}*(1.15)$.

$$f_b = \frac{h_s}{n}\left(\frac{1-e_i}{e_i}\right)\left(\frac{e_{i0}}{e_{c0}}\right)^{\beta}\left(\frac{-trT_s}{h_s}\right)^{1-n}\left[3 + a^2 - \sqrt{3a}\left(\frac{e_{i0}-e_{d0}}{e_{c0}-e_{d0}}\right)^{\alpha}\right]^{-1} \quad (19)$$

$$f_s = \frac{h_s}{n}\left(\frac{1-e_i}{e_i}\right)\left(\frac{e_i}{e}\right)^{\beta}\left(\frac{-trT_s}{h_s}\right)^{1-n}\left[3 + a^2 - \sqrt{3a}\left(\frac{e_{i0}-e_{d0}}{e_{c0}-e_{d0}}\right)^{\alpha}\right]^{-1} \quad (20)$$

The parameters *hs* and *n* were acquired from consolidation loading curves (Figure 9, 10 and 11). The parameter *n* controls the curvature of oedometric curve and *hs* controls the overall slope of oedometric curve (Mašin, 2011). The parameter n can be calculated from

$$n = \frac{\ln\left(\frac{e_1 C_{c2}}{e_2 C_{c1}}\right)}{\ln\left(\frac{p_{s1}}{p_{s2}}\right)} \quad (21)$$

Where mean stresses p_{s1} and p_{s2} can be calculated from axial stresses using the Jacky´s formula K_0=1-sin φ'_C and e_1 and e_2 are the void ratios corresponding to the stresses p_{s1} and p_{s2}.

$$C_c = \frac{\Delta e}{\Delta \ln p_s} \quad (22)$$

$$p_s = \sigma'_z \frac{(1+2K_0)}{3} \quad (23)$$

The parameter *hs* can then be obtained from

$$h_s = 3p_s\left(\frac{ne}{C_c}\right)^{\frac{1}{n}} \quad (24)$$

Where C_c is a secant compression index calculated from limit values (see Figure 6 of Herle & Gudehus, 1999) of the calibration interval p_{s1} and p_{s2}; *ps* and *e* are averages of the limit values of *p* and *e* for this interval.

Parameters α and β (Mašin, 2011) control independently different aspects of soil behavior, the parameter β controls the shear stiffness and α controls the peak friction angle.

For obtaining the final hypoplasticity parameters α, β, *n* and *hs* a calibration process using the SoilTest option of PLAXIS was implementedsee Figure. The parameters can be calibrated (Reference Manual of PLAXIS, 2012) by comparing the real lab results of triaxial and consolidation tests, against its finite element simulations until resemble is reached.

The values of void ratio (e_{c0}, e_{d0} and e_{i0}) and critical friction angle ($\varphi'c$) remained constant through all the calibration process. For simulation and evaluation, the initial void ratio (e_i) parameter corresponds to the simulated test.

The preliminary values of *hs* and *n* were obtained by using Equations 21 and 24. And the results of the densest sample (Table 7) were chosen since some similarity was observed with the lab results (compared to loosest state).

At the beginning of the calibration process (Table 13) α = 0.1 and β = 1 were constant (Constitutive modelling and parameter determination, 2012).

For simulation and evaluation, two drained triaxial test were chosen. The first one corresponds to test 2 (see Figure 7) of the undisturbed sample (normally consolidated). The second one belongs to test 3 (see Figure 8) of the remolded samples (dense sample) using the Proctor test (ASTM D-1557). Also test 2 (see Figure 11) of load-unload consolidation test; test 2 (see Figure 9) of load consolidation test in the loosest state and test 1 (see Figure 10) in a dense state were used.

With the help of the consolidation and triaxial lab results, the values of *hs*, *n*, α and β were proven until resemblance of the model with reality was achieved. In Table 14 are the values of parameters used during the calibration process for hypoplasticity (10 combinations of parameters were verified).

In Table 15 the final hypoplasticity parameters used for simulation are presented.

PLAXIS has an optimization module, where the calibration process is automatic, but during the development of the research it was not available.

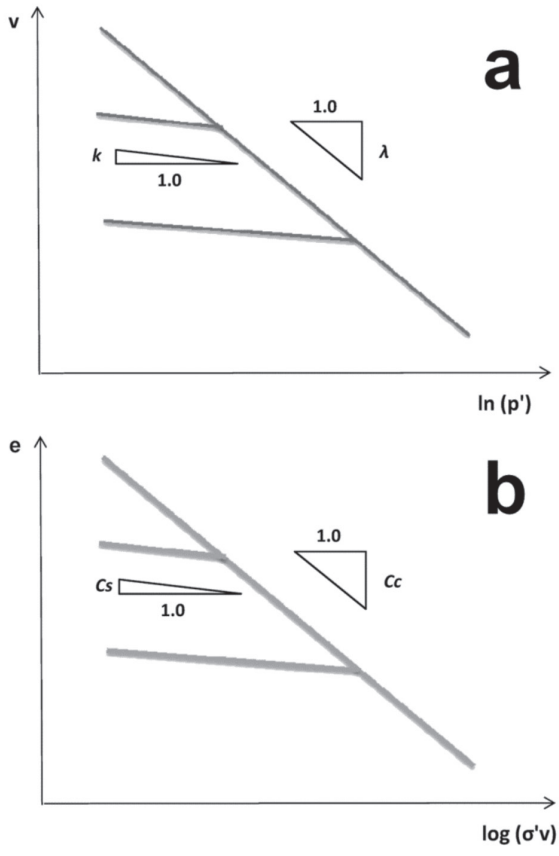

Figure 12. Typical consolidation load-unload tests

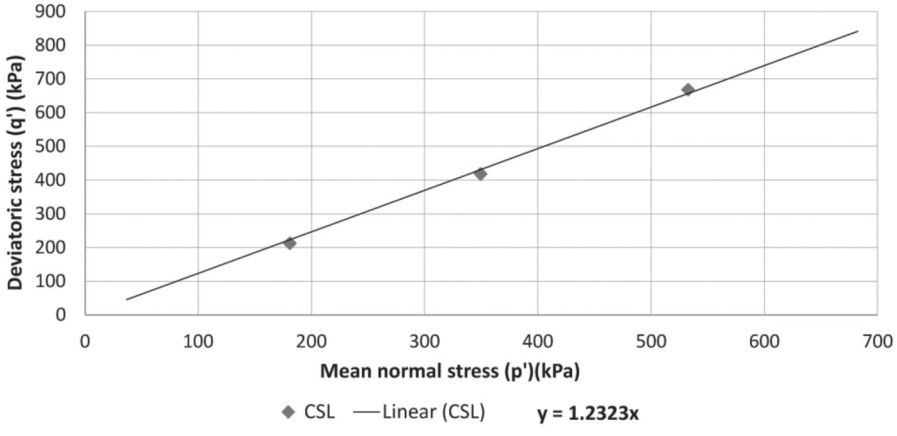

Figure 13. Critical State Line build with the results of undisturbed triaxial tests

Table 9. Results of load-unload consolidation tests.

Test 1		Test 2		Test 3		Test 4	
Stress (kPa)	**Void Ratio**	**Stress (kPa)**	**Void Ratio**	**Stress (kPa)**	**Void Ratio**	**Stress (kPa)**	**Void Ratio**
0	1.9	0	1.93	0	1.83	0	1.83
62.32	1.77	62.52	1.72	62.72	1.58	62.92	1.6
124.65	1.7	125.04	1.64	125.44	1.49	125.84	1.51
249.29	1.63	250.08	1.56	250.88	1.42	251.67	1.44
498.59	1.53	500.17	1.47	501.75	1.32	503.35	1.34
249.29	1.54	250.08	1.48	250.88	1.33	251.67	1.35
124.65	1.55	125.04	1.48	125.44	1.34	125.84	1.36
62.32	1.55	62.52	1.49	62.72	1.35	62.92	1.36
124.65	1.55	125.04	1.49	125.44	1.34	125.84	1.36
249.29	1.54	250.08	1.48	250.88	1.33	251.67	1.35
498.59	1.51	500.17	1.45	501.75	1.31	503.35	1.33
997.18	1.42	1000.34	1.36	1003.51	1.21	1006.7	1.24
1495.77	1.37	1500.5	1.31	1505.26	1.15	1510.05	1.18
997.18	1.37	1000.34	1.31	1003.51	1.16	1006.7	1.19
498.59	1.38	500.17	1.32	501.75	1.17	503.35	1.2
249.29	1.39	250.08	1.33	250.88	1.17	251.67	1.21
0	1.42	0	1.37	0	1.2	0	1.24

Table 10. Parameters used for the Modified Cam Clay model.

Tests Conditions	Load Index (λ)	Unload Index (ϰ)	Tangent of CSL (M, graphic)	Poisson Modulus (υ)
Normally consolidated	0.12	0.00851	1.23	0.29
Overconsolidated	0.12	0.00851	1.23	0.46

Table 11. Void ratio results made for TBJ in the loosest state to obtain the maximum void ratio.

Test	1	2	3	4	5	6	7	8	Average
Maximum Void Ratio	1.9	1.93	1.83	1.83	1.95	2.06	1.87	1.84	**1.9**

Table 12. Minimum Void ratio results made for TBJ in the densest state to obtain minimum void ratio.

Test	1	2	Average
Minimum Void Ratio	1.1	1.12	**1.11**

Table 13. Parameters used at the beginning of the calibration process of Hypoplasticity

Øc	hs	n	edo	eco	eio	α	β
30.9	69031.21	0.59	1.11	1.9	2.19	0.1	1

Table 14. Parameters used during the calibration process for Hypoplasticity model

Hypo 1		**Hypo 2**		**Hypo 3**		**Hypo 4**		**Hypo 5**	
hs=	5000	hs=	6000	hs=	5570	hs=	6000	hs=	6500
n=	0.78	n=	0.78	n=	0.78	n=	0.9	n=	0.85
α=	0.005	α=	0.005	α=	0.005	α=	0.005	α=	0.005
β=	1.35	β=	1.32	β=	1.32	β=	1.32	β=	2.5
Hypo 6		**Hypo 7**		**Hypo 8**		**Hypo 9**		**Hypo 10**	
hs=	8000	hs=	6000	hs=	5570	hs=	5570	hs=	5570
n=	0.9	n=	0.85	n=	0.85	n=	0.85	n=	0.85
α=	0.005	α=	0.005	α=	0.005	α=	0.005	α=	0.005
β=	1.32	β=	2.5	β=	2.5	β=	2	β=	2.35

Table 15. Parameters used for the Hypoplasticity model.

Øc	hs	n	edo	eco	eio	α	β
30.9	5570	0.85	1.11	1.9	2.19	0.05	2.35

3. RESULTS AND CONCLUSIONS

The results of comparing triaxial lab results vs. the outcomes of the models Mohr-Coulomb, Modified Cam Clay and Hypoplasticity (see Table 3, 10 and 15) using PLAXIS is shown below.

In Figure 14 the undisturbed triaxial test and simulations are shown. Modified Cam Clay and Hypoplasticity are closer to the results obtained in the laboratory. Mohr-Coulomb reaches the critical state close to the real value, but with a much lower deformation. The elastic section detach from the lab results since the model presents a plastic failure. The elastic range of the real lab results is very small if compared with the Mohr-Coulomb results.

In Figure 15 the dense triaxial test and simulations are shown. The Modified Cam Clay doesn't simulate the peak caused by the overconsolidation of the soil; the critical state is reached, but after great deformation. Mohr-Coulomb only shows failure in the peak but later (due to its limitations) as deformation increases it does not tend toward the critical state, but remains constant at the point of failure. The Hypoplasticity model has a closer behavior with the lab results. It simulates the peak, but when the deformation increase the stress fall below the critical state. In the laboratory the critical state was not reached in the densest state, since more deformation was needed in the triaxial test.

In Figure 16 the loose consolidation test and simulations are shown, and the models have dissimilar results with the lab data. Modified Cam Clay has a similar curvature as the laboratory results but is shifted in the deformation axis. Hypoplasticity and Mohr-Coulomb don't have a curvature, but the last one is farther from the real results. Both models show an elastic behavior.

In Figure 17 the dense consolidation test and simulations are shown. Comparing the lab data with the models results is possible to note that the Modified Cam Clay and Mohr-Coulomb are not close to the laboratory results; both have extreme soft and rigid boundaries respectively. The Modified Cam Clay exhibits a curvature as the loose sample explained above. Hypoplasticity is much closer to the lab results in this case.

In Figure 18 the load-unload consolidation test and simulations of loose sample are shown. When comparing the models is concluded that none of them display exactly the real behavior. Hypoplasticity is the closest, but only in the initial section (possible linked to the values of *hs* and *n* that depend of the chosen stress range); but with large stresses the results detach from reality. Also the load and unload sections show important changes in the deformation axis. Modified Cam Clay represents well the laboratory results (including loading and unloading sections) but is shifted in the deformation axis. This could be linked to the parameters λ and $\varkappa$ (see Figure 12) that represent the load and unload slopes. The Mohr-Coulomb because of its limitations is only represented by a sloping line (elastic behavior) and it's unable to simulate loading and unloading behavior.

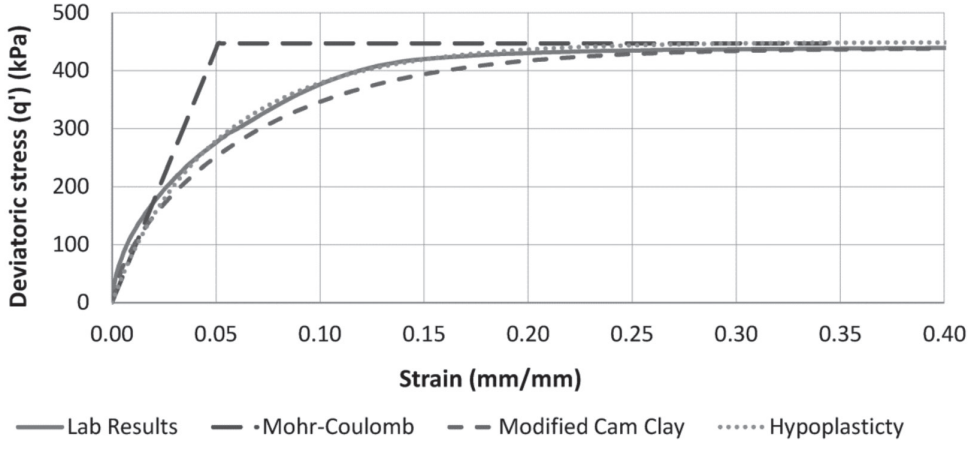

Figure 14. Simulation of undisturbed triaxial test (Test 2)

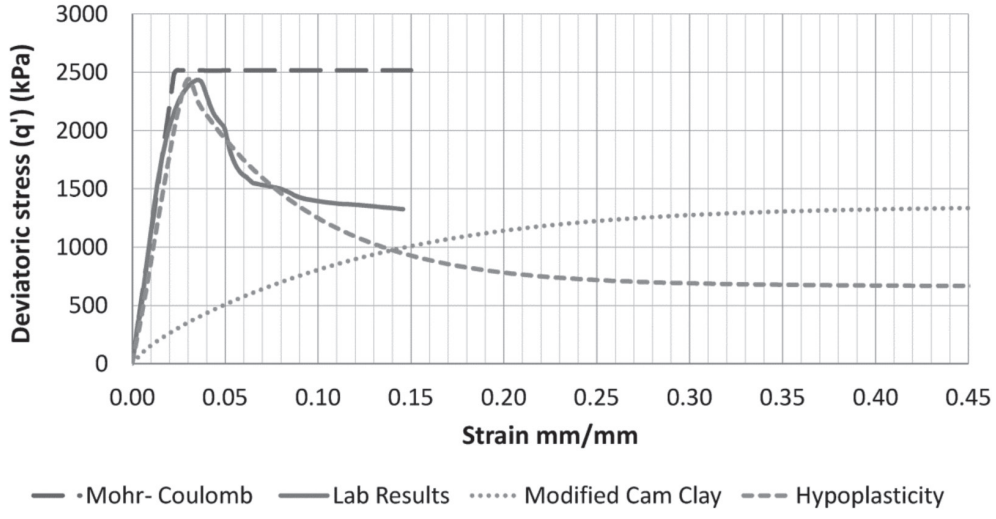

Figure 15. Simulation of dense triaxial test (Test 3)

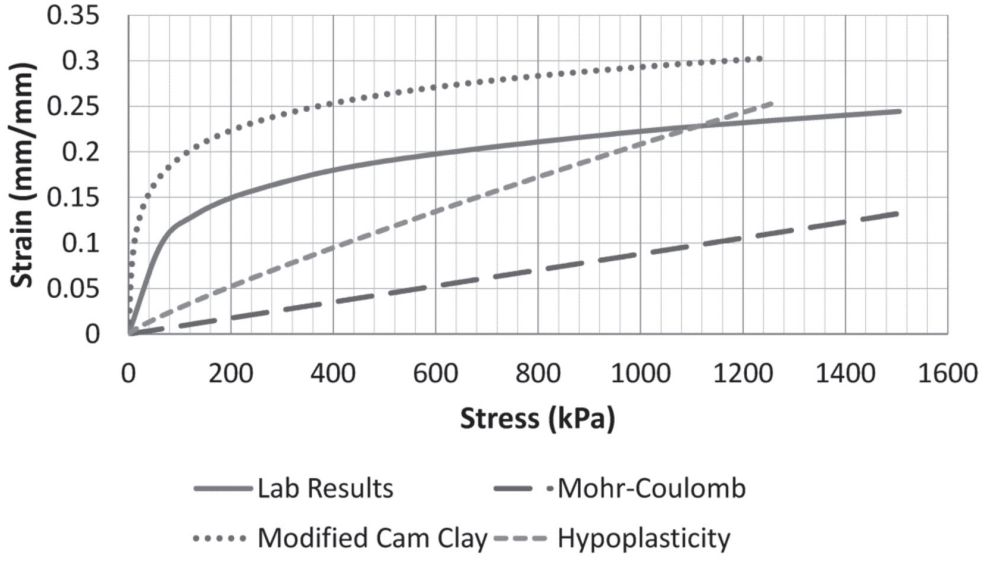

Figure 16. Simulation of consolidation test in a loose sample (test 2)

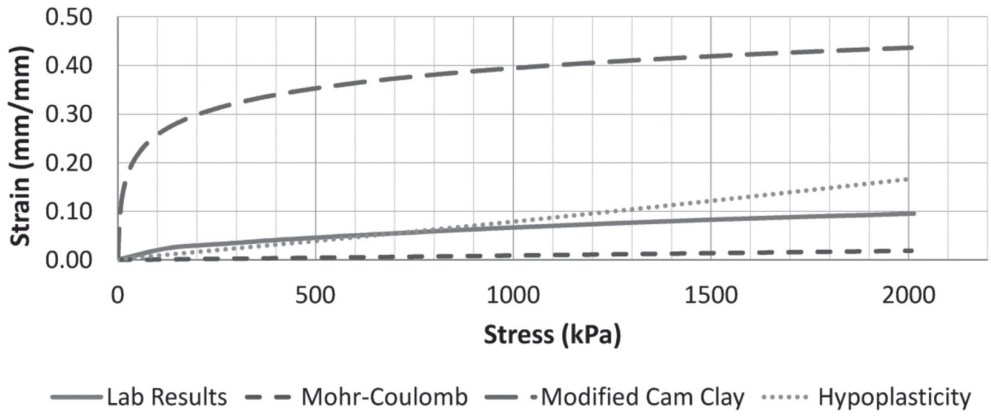

Figure 17. Simulation of consolidation test in a dense sample (Test 1)

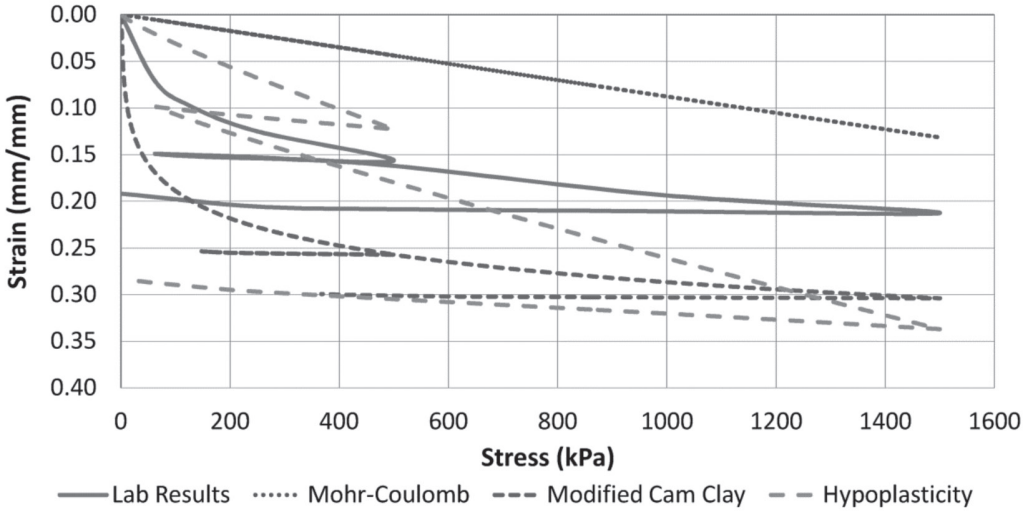

Figure 18. Simulation of consolidation load-unload test in a loose sample (Test 2)

4. CONCLUSIONS AND RECOMMENDATIONS

- In this paper three constitutive models (Mohr-Coulomb, Modified Cam Clay and Hypoplasticity) were used to simulate and compare laboratory results of a volcanic tephra, looking for a model that resembles reality. Tierra Blanca Joven (TBJ) is the most problematic soil in the MASS. The urban areas resting on top of it or close to the streams are prone to mass wasting processes and collapse.
- With the Mohr-Coulomb model (used in the geotechnical designs in El Salvador) in the triaxial tests the values of ultimate or critical stress were close to the real results, but other stress-strain combinations were unrealistic. When compared with the consolidation results the model didn´t describe the real behavior as only an elastic behavior was observed. Mohr-Coulomb has some improvements (increase of cohesion with deep, cut-off tension). This model is only recommended for preliminary design.
- The Modified Cam Clay model results were similar for the undisturbed triaxial test. For the undisturbed consolidation tests the model exhibit a similar tendency like the lab results, but shifted in the strain axis. For the overconsolidated triaxial and consolidation tests significant differences were observed. It is recommended to make load-unload consolidation tests for overconsolidated samples to obtain the model parameters for comparison.
- Good results were obtained with the Hypoplasticity model for sands in the triaxial tests, but in the overconsolidated sample as the strain increased the stress was below the critical stress and didn´t reach it. Hypoplasticity in the consolidation tests cannot simulate the curvature and only in the overconsolidated sample the results are close to the laboratory value. For the load-unload test only the initial section resembles the actual data, this may be related to hs and n values are only valid for a certain range (in this case from 82-660kPa). Other values of loading and unloading sections do not correspond with the results obtained in the tests. Better results to obtain the parameters n, hs, α and β can be expected if an optimization module is used (e.g. PLAXIS) where the calibration process is automatic.
- If compared with others hypoplasticity parameters of sands (Mašin, 2011), the TBJ (sandy silt) results have some differences (see Table 16), especially in n, void ratios and α.
- More tests are necessary to build a strong database of parameters for a chosen model, since soils show strong heterogeneity. The present research has a limited quantity of tests that belongs to one fall layer of unit G of TBJ in the proximal zone. It is recommended to gather more information for more representative parameters or to make a zoning with them.
- The results obtained indicate the necessity to keep searching for a model that fits better the behavior of the soils in El Salvador. The constitutive models are used on finite element software to simulate the behavior of a soil mass (slope stability, bearing capacity, etc.). Using a proper model can improve the performance of designs of foundations, walls, slopes and buildings.
- In El Salvador during the two seasons of the year (summer and rainy season) the groundwater level remains more than 35 m deep in most urban areas (Rolo et al., 2004), this means that most of the soils in the country are unsaturated (presence of water, air and soil) and there are capillary forces acting on the soil structure making that an "apparent cohesion" or suction increases the soil strength, which disappears when saturated or during an strong earthquake/ vibration. Wetting of the soils is likely to take place following construction development, because evaporation is reduced by covering the ground surface with a structure and the failure of water pipelines (Houston, Houston, Zapata & Lawrence, 2001).
- Other possibilities of Hypoplasticity models that can be verified are the models for clays and unsaturated soils (Mašin, 2005; Mašin &Khalili, 2008, 2012). Different authors have proposed other models for unsaturated soils (Murray & Sivakumar, 2010). To prove the proposed models special equipment are needed for unsaturated soils (e.g. triaxial, oedometer, shear box, ring shear). Hoyos, Laloui & Vasallo (2008) present the

current methods in laboratory testing using unsaturated soils cylindrical triaxial systems, including volume changes and stiffness measuring (including small strain stiffness using resonant columns).

- Regularly, the users of commercial finite element software are restricted to use few (often primitive) models. In order to use (and test) a wide range of models (communication of the soilmodels.info project, 2013), the umat format of the finite element program Abaqus (Abaqus, Inc.) could be suitable, since it can be used directly in Abaqus or Tochnog Professional. This format is already used by many researchers and is well documented. Also PLAXIS has a facility to implement user-defined soil models (stress-strain-time relationship), but also accepts umat subroutines through interface implementations.
- According to Chavez et al. (2013) engineering properties like shear strength, volume change and coefficient of permeability can also be predicted with the soil-water retention curve (SWRC) and properties of the saturated soil. These procedures although approximate are generally adequate and practical for design in unsaturated soils.
- Normally in El Salvador, the geotechnical studies don't use the local name (stratigraphic units according to origin, properties and age, (see Figure 2 of Chavez et al., 2012) to identify the studied layer. This classification is important in order to differentiate and collect knowledge of the general properties and characteristics of each layer. Nowadays, the size (up to 10 cm) of the lithic and pumice pieces in the pyroclastic flows (especially units C, α, β and F) makes it difficult to run

Table 16. Comparison of parameters for Hypoplasticity model.

Soil	Øc	hs	n	edo	eco	eio	α	β
Tierra Blanca Joven (TBJ)	30.9	5570	0.85	1.11	1.9	2.19	0.01	2.35
Hochstetten gravel	36	32	0.18	0.26	0.45	0.5	0.1	1.9
Hochstetten sand	33	1.5	0.28	0.55	0.95	1.05	0.25	1.5
Hostun sand	31	1	0.29	0.61	0.96	1.09	0.13	2
Karlsruhe sand	30	5.8	0.28	0.53	0.84	1	0.13	1
Lausitz sand	33	1.6	0.19	0.44	0.85	1	0.25	1
Toyoura sand	30	2.6	0.27	0.61	0.98	1.1	0.18	1.1
Zbraslav sand	31	5.7	0.25	0.52	0.82	0.95	0.13	1

Note: Adapted from "Determination of material parameters" by D. Mašin, 2011, January, PhD course Hypoplasticity for practical applications in National University of Singapore, Singapore

tests in the available triaxial, shear box and oedometer equipment.

- Other aspects needed to research for TBJ are the conditions that originate the mass movements, erosion, collapse of infrastructure which are connected with moisture change, cementing, weathering, external activities and vibration.

ACKNOWLEDGMENTS

The work has been funded in the framework of cooperation between the Oficina de Planificación del Área Metropolitana de San Salvador (OPAMSS), Czech Technical University in Prague (ČVUT), Civil Engineer School of Universidad de El Salvador (UES), Ayuntamiento de Barcelona, Geólogos del Mundo and Suelos & Materiales Laboratory. Special thanks go to Edgard Peña, Jesus Guerrero, Cesar Elias and Walter Hernandez for assistance during this project. In memory of Lorena Molina.

CONTRIBUTION

As the constitutive models are used into finite element software to simulate the behavior of a soil mass (slope stability, bearing capacity etc.) is important to know the diverse possibilities and their competence. The comparison of different constitutive models with real laboratory data can help to choose which one is the most suitable to simulate the soil behavior.

REFERENCES

Amaya, C.A. &. Hayem E.A (2000). *Introducción al estudio de suelos parcialmente saturados e inicio de la caracterización de la tierra blanca del AMSS*. (Trabajo de graduación para Ingeniería Civil) Universidad Centroamericana José Simeón Cañas, San Salvador.

Anaraki, K. (2008). *Hypoplasticity Investigated Parameter Determination and Numerical Simulation* Master of Science Thesis for obtaining the degree of Master of Science in Geotechnical Engineering at Delft University of Technology, Delft, the Netherlands.

Atkinson, J. (2007). *The mechanics of soils and foundations* (2nd ed.). New York: Taylor & Francis.

Avalos, J.R. & Castro, R.M. (2010). *Caracterización geológica y geotécnica de la unidad "G" de Tierra Blanca Joven*. (Trabajo de graduación Ingeniería Civil) Universidad Centroamericana José Simeón Cañas, San Salvador.

Camacho, J. F. Reyes, O. J., & Bueno, P. B. (2004). Utilización del modelo Cam-Clay Modificado en suelos cohesivos de la sabana de Bogotá. *Ciencia e Ingeniería Neogranadina*, 14, 1-13.

Chávez, J.A., Hernandez, W., & Kopecky, L. (2012). Problemática y conocimiento actual de las tefras Tierra Blanca Joven en el Área Metropolitana de San Salvador, El Salvador. *Revista Geológica de América Central*, 47, 117-132.

Chávez, J. A., Schrofel, J., Valenta, J., Šebesta, J. & Hernandez, W. (2012). Engineering geology mapping in southern part of the Metropolitan Area of San Salvador. *Revista Geológica de América Central*, Vol. 46, 161-178.

Chavez, J.A., Šebesta, J., Kopecky, L., López, R. & Landaverde, J. (2013). Unsaturated volcanic tephra and its effect for soil movement in El Salvador. *Earth Science, 2(2),* 58-65.

Craig, R. F. (2004). *Craig´s soil mechanics* (7th edition). London: Taylor and Francis.

Fredlund, D. G. & Rahardjo, H., (1993). *Soil mechanics for unsaturated soils*. New York : Ed. Wiley-Intescience Publications.

Guzmán, M.A., & Melara, E., (1996). Propiedades ingenieriles del suelo del Área Metropolitana de San Salvador, El Salvador. *Revista ASIA, 122,* 14–22.

Herle, I. & Gudehus, G. (1999). Determination of parameters of a hypoplastic constitutive model from properties of grain assemblies. *Mechanics of Cohesive-frictional Materials*, *5(4)*, 461–486.

Hernández, W. (2004). *Características Geotécnicas y Vulcanológicas de las tefras de Tierra Blanca Joven, de Ilopango, El Salvador.* (Tesis de Maestría en Tecnologías geológicas) Universidad Politécnica de El Salvador, San salvador.

Houston, S., Houston, W., Zapata, C. & Lawrence, C. (2001). Geotechnical engineering practice for collapsible soils. In D. Toll. (Ed.), *Unsaturated soil concepts and their application in geotechnical practice* (pp. 333.355). Dordrecht, The Netherlands: Kluwer Academic Publishers.

Hoyos, L.R, Laloui, L. & Vasallo, R. (2008). Mechanical testing in unsaturated soils. *Geotechnical and Geological Engineering,* 6(26), 675-689.

Mašın, D. (2005).A hypoplastic constitutive model for clays. I*nternational Journal for Numerical and Analytical Methods in Geomechanics*, 29, 311–336.

Mašin, D. (2011, January). *Determination of material parameters*. PhD course Hypoplasticity for practical applications in National University of Singapore, Singapore.

Mašın, D. & Khalili, N. (2008). A hypoplastic model for mechanical response of unsaturated soils, *International Journal for Numerical and Analytical Methods in Geomechanics, 32,* 1903–1926.

Mašın, D. & Khalili, N. (2012). A thermomechanical model for variably saturated soils based on Hypoplasticity *International Journal for Numerical and Analytical Methods in Geomechanics, 36,* 1461-1485.

Molina, B.M., Pérez, G.N. & Vásquez, M.E (2009). *Caracterización geotécnica de las tefras Tierra Blanca Joven: unidad "G" en la zona proximal y obras de protección*. (Trabajo de graduación para Ingeniería Civil) Universidad Centroamericana José Simeón Cañas, San Salvador.

Murray, E. & Sivakumar, V. (2010). *Unsaturated soils: A fundamental interpretation of soil behavior.* London: Wiley-Blackwell.

PLAXIS. (2012). *Material Models Manual of PLAXIS*. The Netherlands: Author

PLAXIS. (2012). *Reference Manual of PLAXIS*. The Netherlands: Author

PLAXIS. (2012). *Constitutive modelling and parameter determination*. The Netherlands: Author

Potts, D. M & Zdravković, L. (1999). *Finite element analysis in geotechnical engineering-theory*. London: Thomas Telford Publishing.

Rolo R., Bomer. J.J., Houghton. B.F., Vallance. J.W., Berdousis. P., Mavrommati. C. & Murphy. W. (2004). Geologic and Engineering Characterization of Tierra Blanca Pyroclastic Ash Deposits. In Rose, W.I., Bommer, J.J., López, D.L., Carr, M.J., and Major, J.J. (Eds.), *Natural hazards in El Salvador* (pp.55-67). Boulder, USA: Geological Society of America.

Von Wolffersdorff, P. A.(1996) A hypoplastic relation for granular materials with a predefined limit state surface. *Mechanics of Cohesive-Frictional Materials, 3(1)*,251-271.

ABOUT THE AUTHORS

Jose Alexander Chavez Hernandez
Czech Technical University in Prague, Oficina de Planificacion del Area Metropolitana de San Salvador, El Salvador.Doctorante en Czech Technical University in Prague, Faculty of Civil Engineering, Department of Geotechnics.Salvador.
Email: jalexanderchavez@gmail.com

José Miguel Landaverde Quijada
Universidad de El Salvador, El Salvador. Jefe de Departamento de Geotecnia Escuela de Ingeniería Civil, Universidad de El Salvador.
Email: Jmlq30@yahoo.com.mx

Oscar Edgardo Ayala Valdez
Universidad de El Salvador, El Salvador.Estudiante de escuela de civil de la Universidad de El Salvador (UES). Email: oscarvaldez.oeav@gmail.com

Lesly Emidalia Mendoza Mejia
Universidad de El Salvador, El Salvador. Profesor Universitario II de Geotecnia Escuela de Ingeniería Civil, Universidad de El Salvador.
Email: lesly.mendoza@fia.ues.edu.sv